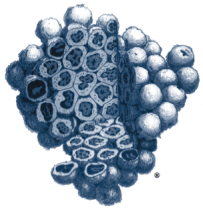

STEM CELLS®

No Evidence of Clonal Dominance in Primates up to 4 Years Following Transplantation of Multidrug Resistance 1 Retrovirally Transduced Long-Term Repopulating Cells

Farastuk Bozorgmehr, Stefanie Laufs, Stephanie E. Sellers, Ingo Roeder, Werner J. Zeller, Cynthia E. Dunbar and Stefan Fruehauf

Stem Cells 2007;25;2610-2618; originally published online Jul 5, 2007;
DOI: 10.1634/stemcells.2007-0017

STEM CELLS®

THE STEM CELL NICHE

No Evidence of Clonal Dominance in Primates up to 4 Years Following Transplantation of Multidrug Resistance 1 Retrovirally Transduced Long-Term Repopulating Cells

FARASTUK BOZORGMEHR,[a] STEFANIE LAUFS,[b] STEPHANIE E. SELLERS,[c] INGO ROEDER,[d] WERNER J. ZELLER,[a] CYNTHIA E. DUNBAR,[c] STEFAN FRUEHAUF[e,f]

[a]Research Group Pharmacology of Cancer Treatment, German Cancer Research Center, Heidelberg, Germany; [b]Department of Experimental Surgery Mannheim Faculty, University of Heidelberg, and Molecular Oncology of Solid Tumors Unit, Deutsches Krebsforschungszentrum (*DKFZ*), Heidelberg, Germany; [c]Hematology Branch, National Heart, Lung and Blood Institute, NIH, Bethesda, Maryland, USA; [d]Institute for Medical Informatics, Statistics and Epidemiology, University of Leipzig, Leipzig, Germany; [e]Department of Internal Medicine V, University of Heidelberg, Heidelberg, Germany; [f]Center for Tumor Diagnostics and Therapy, Paracelsus Klinik, Osnabrueck, Germany

Key Words. Gene therapy • Multidrug resistance 1 • CD34+ • Rhesus macaque

ABSTRACT

Previous murine studies have suggested that retroviral multidrug resistance 1 (*MDR1*) gene transfer may be associated with a myeloproliferative disorder. Analyses at a clonal level and prolonged long-term follow-up in a model with more direct relevance to human biology were lacking. In this study, we analyzed the contribution of individual CD34-selected peripheral blood progenitor cells to long-term rhesus macaque hematopoiesis after transduction with a retroviral vector either expressing the multidrug resistance 1 gene (*HaMDR1* vector) or expressing the neomycin resistance (*NeoR*) gene (*G1Na* vector). We found a total of 122 contributing clones from 8 weeks up to 4 years after transplantation. One hundred two clones contained the *G1Na* vector, whereas only 20 clones contained the *HaMDR1* vector. Here, we show for the first time real-time polymerase chain reaction based quantification of individual transduced cell clones constituting 0.0008% ± 0.0003% to 0.0041% ± 0.00032% of primate peripheral blood cells. No clonal dominance was observed. STEM CELLS *2007;25:2610–2618*

Disclosure of potential conflicts of interest is found at the end of this article.

INTRODUCTION

Dose intensity of cytostatic drugs correlates with therapeutic response in hematologic and solid tumors [1]. Hematologic side effects are often dose-limiting and can be overcome by cytostatic drug resistance gene transfer to hematopoietic stem cells (HSCs) in experimental models [2–5]. The *MDR1* gene encodes a 170-kDa membrane-associated drug-efflux pump [6]. This transmembrane pump efficiently effluxes lipophilic cytotoxic substances, including doxorubicin, etoposide, vinca-alkaloids, paclitaxel, and imatinib, conferring resistance to many types of cancer cells [7–9]. Although it could be shown that overexpression of *MDR1* in transgenic mice and transduced murine HSCs leads to drug resistance [4, 10, 11], studies in nonhuman primates and clinical trials have shown no evidence of significant selective advantage so far [12–17]. Failure to demonstrate efficient in vivo selection following retroviral gene transfer in such trials may have been due to inefficient transduction, transgene expression, and conditioning regimes, which have been overcome recently [18–20].

Anxiety was raised regarding further use of *MDR1* gene transfer in human clinical trials following the occurrence of a polyclonal myeloproliferative syndrome in mice after transplantation of marrow cells transduced with a Harvey murine sarcoma virus vector expressing *MDR1* (*HaMDR1*) [21, 22]. In addition, more recent concerns have arisen regarding insertional mutagenesis, based on an interaction between the vector backbone, the transgene, the multiplicity of infection, and the host cells [23]. Therefore, additional studies addressing the safety and feasibility of *MDR1* gene therapy with new transduction and conditioning protocols and in the relevant target cell population are required.

Here, we used a nonhuman primate model with direct relevance to human biology to investigate the safety of *MDR1* gene transfer. A proliferative advantage of *MDR1*-transduced versus *NeoR*-transduced HSCs after 1 year of follow-up was not observed using semiquantitative polymerase chain reaction (PCR) methods [24]. In this work, we quantified for the first time using a fluorescence-based quantitative real-time PCR (QRT-PCR) [25] the contribution of *MDR1*-transduced HSCs to hematopoiesis after a 4-year follow-up not only on a bulk cell population but also on the level of single hematopoietic stem and progenitor cells.

With respect to the safety aspects of gene transfer, we analyzed the integration pattern of the *G1Na* and *HaMDR1*

Correspondence: Stefan Fruehauf, M.D., Center for Tumor Diagnostics and Therapy, Paracelsus Klinik, Am Natruper Holz 69, 49076 Osnabrueck, Germany. Telephone: 49-541-9663040; Fax: 49-541-9663046; e-mail: prof.stefan.fruehauf@pk-mx.de Received January 25, 2007; accepted for publication June 18, 2007; first published online in STEM CELLS *EXPRESS* July 5, 2007. 1066-5099/2007/$30.00/0 doi: 10.1634/stemcells.2007-0017

vectors, regarding the occurrence of integrations in oncogenes. An additional aim was to investigate whether primate *MDR1* gene transfer results in the dominance of transduced clones after prolonged periods of follow-up. Since we were not able to perform ligation-mediated PCR (LM-PCR) [26] on all samples because of limited DNA amounts, we established a new, highly sensitive PCR method for detection of vector integration sites using exponential fragment marking (EFRAM).

MATERIALS AND METHODS

Experimental Setup

Animal care, cell collection, transduction, and expansion were performed by Sellers et al. as described [24]. Briefly, 47×10^6 and 34×10^6 CD34-enriched cells from mobilized peripheral blood cells (PBCs) of rhesus macaques M038 and M120, respectively were obtained, split into equal aliquots, transduced with either the *HaMDR1* vector (based on the Harvey murine sarcoma virus) or a control neo marking vector (*G1Na* vector, based on the Moloney murine leukemia virus), and expanded as described [24]. Before transplantation, animals were conditioned with 10 Gy of total body irradiation followed by coincident infusion of both aliquots, containing *HaMDR* and *G1Na*-transduced cells.

Blood samples were taken at different time points, from 8 weeks up to 4 years after transplantation (8, 46, and 50 weeks and 4 years after transplantation for monkey M120; 8, 12, 16, 23, 54, and 58 weeks and 4 years after transplantation for monkey M038) and separated into mononuclear cells (MNCs) and granulocytes [24]. The samples were analyzed with LM-PCR or EFRAM-PCR, depending on the DNA amount of the sample, and then quantified using QRT-PCR.

Detection of Vector Integration Sites

LM-PCR. LM-PCR and integration site analysis were performed as described previously [26]. Briefly, 2,500 ng of DNA was digested using restriction enzyme BsmAI (New England Biolabs, Ipswich, MA, http://www.neb.com); after purification of the digest a one-step amplification reaction was performed using the long terminal repeat (LTR)-specific biotinylated primer HaRV292bio (5′biotin-CAGATGCGGTCCAGCCCTCA-3′). After purification and enrichment for biotin-marked fragments with streptavidin-coated paramagnetic beads (Dynal, Oslo, Norway, http://www.dynalbiotech.com), adapter ligation was performed using a blunt-end adapter oligo-cassette (Clontech, Palo Alto, CA, http://www.clontech.com). Amplification of the fragments was performed using the primers HaRV292 (5′-CAGATGCGGTCCAGCCCTCA-3′) and AP1 (5′-GTAATACGACTCACTATAGGGC-3′). Subsequently, nested PCR was performed using the primers HaRV111 (5′-TCCTGACCTTGATCTGAAC-3′) and AP2 (5′-ACTATAGGGCACGCGTGGT-3′). All PCR products were cloned into the *pCR4* plasmid vector (Invitrogen, Carlsbad, CA, http://www.invitrogen.com) and then sequenced using an ABI Prism Genetic Analyzer 310 (PE Applied Biosystems, Weiterstadt, Germany, http://www.appliedbiosystems.com).

EFRAM-PCR. First, 100 ng of DNA was digested using 80 U of HhaI (New England Biolabs) for 1 hour at 37°C. After purification of the digest (Mini Elute reaction cleanup kit; Qiagen, Hilden, Germany, http://www1.qiagen.com), primers A1 (5′-AGCACTCTCCAGCCTCTCACGGCG-3′) and A3 (5′-CCGTGAGA-3′), 0.45 nmol of each, were allowed to anneal at 55°C for 10 minutes, creating asymmetric adapter cassettes that were ligated to the digested DNA-fragments using 400 U of T4 DNA ligase under incubation for 16 hours at 16°C. T4 ligase was then inactivated at 65°C for 10 minutes. Next, PCR was performed on the ligated fragments using 15 pmol of the biotinylated LTR-specific primer HaRV292bio, 15 pmol of primer A1, 7.5 U of Taq polymerase, 64 nmol of dNTPs, and water to a final volume of 100 μl. Samples were placed in a preheated thermocycler, and a 29 cycle amplification reaction was started using following amplification conditions: 95°C, 1 minute; 63°C, 1 minute; 72°C, 3 minutes; final extension at 72°C for 10 minutes. After purification and paramagnetic enrichment of biotin-marked fragments (Kilobase binder kit; Dynal), PCR amplification of the enriched fragments was performed using the Expand High Fidelity PCR System (Roche Diagnostics, Basel, Switzerland, http://www.roche-applied-science.com) with 15 pmol of the LTR-specific primer HaRV292 and 15 pmol of A1 under the following conditions: 94°C, 2 minutes; 95°C, 15 seconds; 63°C, 1 minute; 72°C, 90 seconds; 68°C, 3 minutes; 30 cycles; final extension at 72°C for 7 minutes. The PCR-product was diluted 1:50, and then nested PCR was performed with 15 pmol of LTR-specific primer HaRV111 and 15 pmol of primer A1 under the conditions mentioned above, except with reduced cycle number ($n = 28$) and a primer annealing temperature of 55°C. All PCR products were cloned into the *pCR4* plasmid vector (Invitrogen) and then sequenced using an ABI Prism Genetic Analyzer 310 (PE Applied Biosystems). A scheme showing the principle of the EFRAM-PCR is displayed in Figure 1A.

Assignment of Clone Identity. The first 110 bases of the LTR sequences of both vectors are identical, except for the base at position 68, which is thymidine in the *HaMDR1*-LTR and cytosine in the *G1Na*-LTR. To confirm that the likelihood of each vector being detected by LM-PCR and EFRAM-PCR was the same, we designed primers that aligned to this equal sequence on both vector LTRs and led to amplification of LTR sequences of equal length. Using the difference of the LTR sequences in position 68, we were able to definitely allocate each identified clone to one vector or the other after sequencing.

Integration Analysis. The sequences detected using LM-PCR and EFRAM-PCR were first viewed using Chromas 2.23 software (Technelysium Pty. Ltd., Helensville, Queensland, Australia, http://www.technelysium.com). An integration site was considered valid only when the sequence of interest was flanked by the LTR sequence on one side and the adapter sequence on the other side. Integration analysis was performed using the IntegrationMap task (available online at http://genius.embnet.dkfz-heidelberg.de/menu/biounit/open-husar or for all services after registration for an account at http://genome.dkfz-heidelberg.de), as described by Giordano et al. [27]. Briefly, IntegrationMap first runs a MEGABLAST analysis using the NCBI 35b assembly as described [28]. The location (i.e., information about chromosomal position, contig position, and strand) is then computed. Using an application program interface of Ensembl.org (http://www.ensembl.org/Homo_sapiens), the positions of the next gene (i.e., its transcription start site), the next repetitive elements (e.g., short interspersed nucleotide elements [SINE], long interspersed nucleotide elements [LINE], simple repeats, and LTR elements), and the next CpG island are computed, and their distances to the exact integration base are calculated. If the integration position is localized within a gene, the exon or intron number is also displayed.

Real-Time Quantitative PCR

We used a fluorescence-based real-time quantitative PCR [25]. Absolute quantitation of input DNA was accomplished by generating a standard curve with serial dilutions of the plasmid-cloned target DNA and then comparing the signals obtained from samples with unknown amounts of vector or clone-specific DNA to the standard curve (User's Manual, ABI Prism 7700 Sequence Detection System; PE Applied Biosystems). Concentration of each plasmid solution was determined as a mean of three A_{260} photometric measurements and converted to the number of copies using the molecular weight of the plasmid. We made serial dilutions of the plasmids in the range of 10^0–10^5 copies per microliter. To minimize the amount of plasmid DNA absorbed to the wall of the tube, a constant amount of carrier DNA (salmon sperm DNA, 10 ng/μl) was added to the diluted plasmids. Dilutions were performed once, and sufficient numbers of aliquots of each dilution of the chosen plasmid standard curve were stored at −20°C. All real-time reactions were performed using new aliquots to minimize degradation of DNA because of repeated freeze/thaw cycles. A dilution series was only considered as acceptable if the correlation coefficient of the standard curve was more than 0.98 and the Ct values increased by approximately 3 for each 10-fold dilution, as recommended by PE

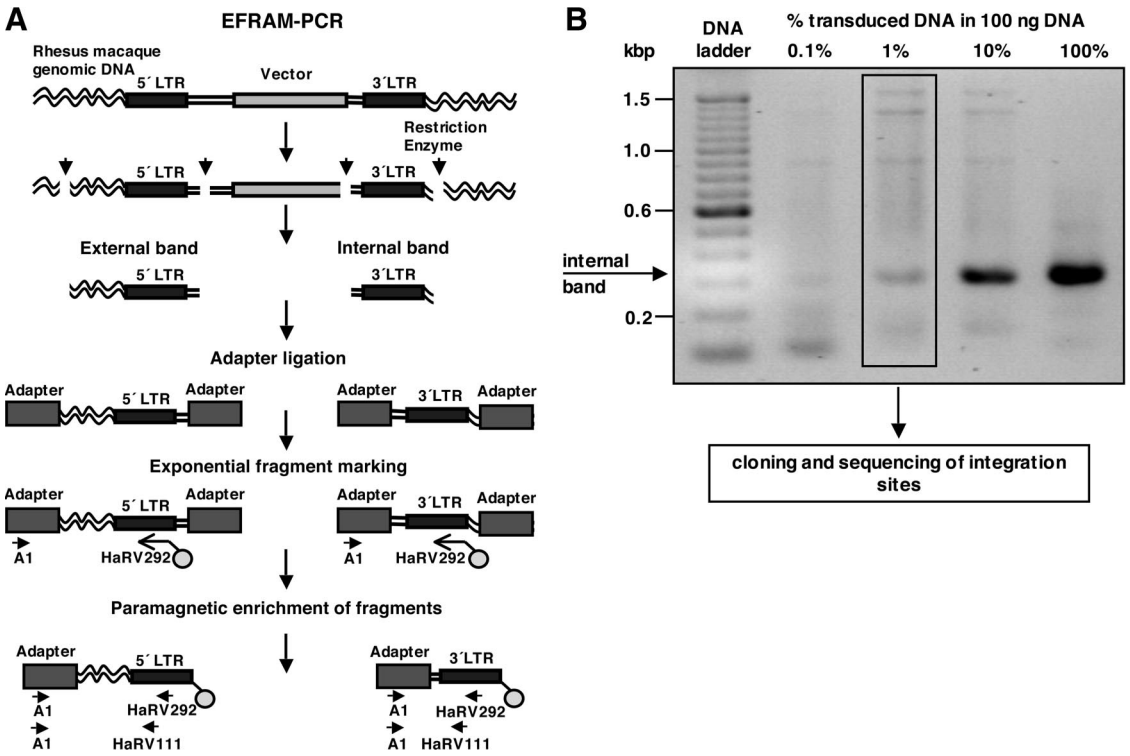

Figure 1. EFRAM-PCR. **(A):** EFRAM-PCR technique. Rhesus macaque genomic DNA was isolated. A restriction enzyme digest (↓) was performed. An adapter oligo-cassette was ligated to flanking DNA. Fragments containing LTR-genomic DNA junctions were marked with a biotinylated LTR-specific primer (HaRV292-bio) and enriched by streptavidin-coated paramagnetic beads. Other DNA fragments were flushed away. Nested PCR was performed (A1, adapter-specific primer; HaRV292/HaRV111, LTR-specific primers). **(B):** Agarose gel electrophoresis of PCR products obtained with EFRAM-PCR. EFRAM-PCR was performed on serial dilutions of the cell line HT1080 containing 0.1%–100% retrovirally transduced DNA in a background of untransduced DNA. The arrow indicates the internal band that represents the PCR product amplified from the proviral 3′LTR. With increasing amounts of vector-containing DNA, we observed increasing signal intensity of the internal band expected at 300 base pairs. To confirm that the band was specific, we cloned and sequenced the obtained band of the 1% dilution sample. Mock controls were negative. Abbreviations: EFRAM-PCR, exponential fragment-marking polymerase chain reaction; kbp, kilobase pairs; LTR, long terminal repeat.

Applied Biosystems (User's Manual, ABI Prism 7700 Sequence Detection System). The Ct value is defined as the cycle number at which a significant increase in the fluorescence signal is first detected. The PCR efficiency was deduced from each standard curve by ABI Prism 7700 software and expressed as $E = 10^{-1/s} - 1$, where s is the curve slope.

To assess the total copy number of *G1Na* and *HaMDR1* vector DNA in a sample and the total amount of DNA in the sample, three reference standard curves were generated using the *NeoR* gene, the *MDR1* gene [29], and the rhesus macaque β-2-microglobulin gene (*rhB2M*). The *pcDNA3.1*(−) plasmid (Invitrogen) and the *SFβm1* plasmid [30] were used for the *NeoR* and the *MDR1* dilution series, respectively. For the *rhB2M* standard curve, a part of exon 2 of the gene was PCR-amplified using the Expand High Fidelity PCR System (Roche Diagnostics) together with 15 pmol of each primer, 5′-GTACTCCAAAGATTCAGGTT-3′ and 5′-CACTTAACTGTC-CTGGGC-3′ (based on the *rhB2M* sequence, GenBank accession no. AY349163) [31], by using the following PCR regimen: 94°C, 15 seconds; 52°C, 30 seconds; 72°C, 90 seconds; 30 cycles.

To assess the copy number of a single clone, the standard curves were constructed by diluting plasmids containing the LM-PCR or EFRAM-PCR product of this clone [29]. This copy number is the absolute copy number of the clone, which can be displayed as the percentage of the clone to the total DNA and as the percentage of the clone to the overall gene modified population (supplemental online Fig. 1).

Primers and Probes. Primers and TaqMan 5′ Fam/3′ TAMRA probes were designed using Primer Express software (version 1.5; PE Applied Biosystems). Primers were as follows: *NeoR,* 5′-CTT-GGGTGGAGAGGCTATTCG-3′ and 5′-CCTCGTCCTGCAGT-TCATTCA-3′; *rhB2M*, 5′-CAGGTTTACTCACGCCATCCA-3′ and 5′-ACTTTTCCCATTTTCTCTCCATTC T-3′; and LTR, 5′-TCCTGACCTTGATCTGAACTTCTCT-3′. The following sequences were used as probes: *NeoR* probe, 5′-CAAGACCGACCT-GTCCGGTGCC-3′; *rhB2M* probe, 5′-TCCAGACACATAGCAATT-CAGGAAATTTGGCT-3′; *G1Na*-LTR probe, 5′-CATGCCTTG-CAAAATGGCGTTACTTAAGCTAGC-3′; and *HaMDR1*-LTR probe, 5′-CATGCCTTGTAAAATGGCGTTACTTAAGCTAGC-3′. *MDR1* primers and probe were designed as described previously [3]. Sequences of unique primers binding to the flanking rhesus DNA were designed for 18 integration site sequences.

PCR Amplification. QRT-PCR was performed on an ABI Prism 7700 Sequence Detection System instrument (PE Applied Biosystems). PCR amplification was performed as described before [29]. The reactions were performed two times in triplicate.

Cross-Reactions. To measure the specificity of each clone-specific reverse primer, a plasmid mix was generated for each clone using 450 ng of untransduced rhesus macaque DNA as a background and 10 copies of each plasmid containing an integration site except the one that served as template for the primer design. Then, QRT-PCR was performed on the amplification mix as described above, with the specific reverse primer for the clone missing in the plasmid mix. Untransduced rhesus macaque DNA served as a "no amplification" control (NAC), and H_2O served as a "no template" control (NTC).

Statistical Analysis. PCRs were performed two times in triplicate for a clone (A) and the vector (B). The means of the triplicates (A_1 and B_1) and the appropriate SEM (a_1 and b_1) in the first PCR run as well as the means of the triplicates (A_2 and B_2) and the appropriate SEM (a_2 and b_2) in the second PCR run on each sample were calculated. These means represent the absolute copy numbers of a clone or a vector, respectively. The relative proportion of a clone within the overall population of gene modified cells was estimated

Table 1. Number of clones identified, mapped, and quantified in monkey M120 and M038

	HaMDR1	G1Na	Total
M120	8	59	67
M038	12	43	55
Total	20	102	122
Mapped clones	15	72	87
Quantified clones	2	16	18

by the ratio of the absolute copy numbers of the clone and the vector for each PCR performance, that is, $D_1 = A_1/B_1$ and $D_2 = A_2/B_2$. From these two ratios, the average percentage of clone contribution $D = 0.5 \times (D_1 + D_2)$ was determined. The SE (d) for this average percentage D was calculated using the following formula: $d = 0.5 \times \sqrt{d_1^2 + d_2^2}$ with $d_1 = 1/B_1^2 \times \sqrt{A_1^2 \times b_1^2 + B_1^2 \times a_1^2}$ and $d_2 = 1/B_2^2 \times \sqrt{A_2^2 \times b_2^2 + B_2^2 \times a_2^2}$ [32].

The percentage of a clone's contribution to the total DNA, which represents the contribution of a clone to total primate hematopoiesis, and the percentage of the vector to the total DNA, which represents the overall gene modified population, were estimated similarly. We determined two different CV values: the intraexperimental CV, showing the degree of variation between the same samples (triplicates) in one experiment, and the interexperimental CV, showing the extent of variation in repeated experiments.

RESULTS

Our aim was to investigate whether *MDR1* gene transfer results in the dominance of transduced clones after prolonged periods of follow-up. To this end, we compared the in vivo contribution of *MDR1* gene-transduced versus *NeoR* gene-transduced rhesus macaque hematopoietic repopulating cells up to 4 years after autologous transplantation.

Using monkeys M038 and M120, 47×10^6 and 34×10^6 CD34-enriched cells from mobilized PBCs, respectively, were obtained, transduced, and then expanded as described by Sellers et al. [24]. At the end of culture, the total cell number had expanded 40- and 37-fold for the *HaMDR1*-transduced cells and 47- and 67-fold for the *G1Na*-transduced cells [24]. These cells were then transplanted after total body irradiation [24].

Detection of Vector Integration Sites

LM-PCR is a suitable method to amplify multiple retroviral integration sites from at least 2,500 ng of genomic DNA [26]. Because of the limitation set by small amounts of DNA in our samples, we modified this method. After optimization of the EFRAM-PCR method on transduced cell line clones, we could detect 1 ng of transduced DNA in a background of 99 ng of untransduced DNA (Fig. 1B). The HT1080 cell line used has two vector integration sites per cell, which are located at chromosomes 1q41 and 3q21 (GenBank accession nos. AC092015 and AC083798, respectively). The bands bigger than 600 kb appearing in the samples with a low content of transduced DNA were nonspecific. This explains why with higher amounts of marked DNA they became less prominent: there were more specific binding sites available for the primers in the samples containing 10% and 100% transduced DNA, so nonspecific binding of the primers occurred less frequently.

Using LM-PCR and EFRAM-PCR, we detected a total of 122 unique contributing clones in granulocytes and mononuclear cells from 8 weeks up to 4 years after transplantation. Twenty samples were analyzed, 6 with LM-PCR and 14 with EFRAM-PCR. We used EFRAM-PCR only in samples with limited DNA availability. One hundred two clones contained the

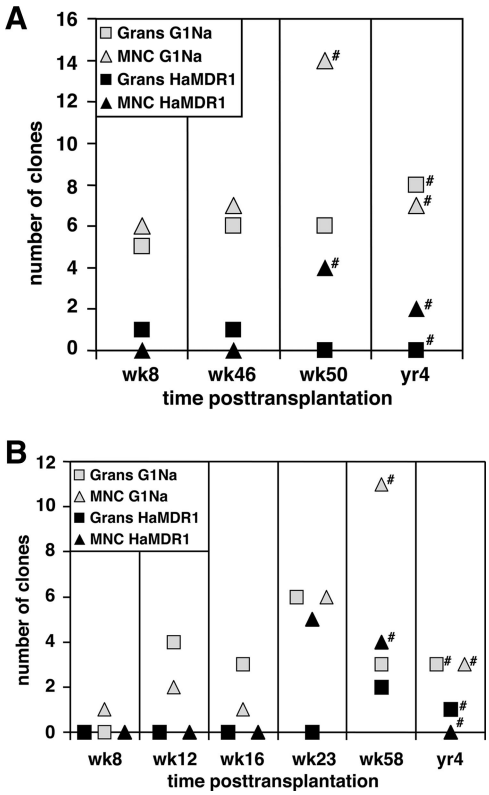

Figure 2. Number of clones identified at different time points after transplantation. **(A):** Monkey M120; **(B):** Monkey M038. The clones were arranged according to integrated vector (gray, *G1Na*; black, *HaMDR1*) and analyzed fraction (□, Grans; △, MNCs). #, clones detected with ligation-mediated polymerase chain reaction (PCR). All other clones were detected with exponential fragment-marking PCR. Abbreviations: Grans, granulocytes; MNC, mononuclear cell; wk, week; yr, year.

G1Na vector, whereas 20 contained the *HaMDR1* vector. In monkey M120, the ratio of *HaMDR1* clones to *G1Na* clones was 1/7.4 (8/59); in monkey M038, the ratio was 1/3.6 (12/43). The total number of identified clones for each monkey, vector, and PCR method is shown in Table 1 and supplemental online Table 1. The number of clones found at different time points for each animal is shown in Figure 2A (M120) and 2B (M038), which also shows the number of clones in granulocytes and in mononuclear cells (primary T-lymphocytes), respectively. The number of identified *G1Na* clones was at each time point higher than the number of identified *HaMDR1* clones, regardless of the PCR method used.

Quantitation of Transgenes

We used a fluorescence-based real-time quantitative PCR method to determine the contribution of the two vectors to hematopoiesis. The real-time quantitative PCR method is an established and widely used method to quantify the copy number of a sequence in a very small starting amount of DNA. The method is highly sensitive and specific [33–36]. A recent study detected and quantitated contribution levels of 0.00001% to 0.001% of a single clone analyzed with QRT-PCR in a polyclonal background [37].

The absolute quantitation assay was chosen to determine the copy number of the samples. Our standard curves showed a correlation coefficient of more than 0.98 and an increase of Ct values by approximately 3 for each 10-fold dilution (supplemental online Figs. 2, 3), as recommended by PE Applied

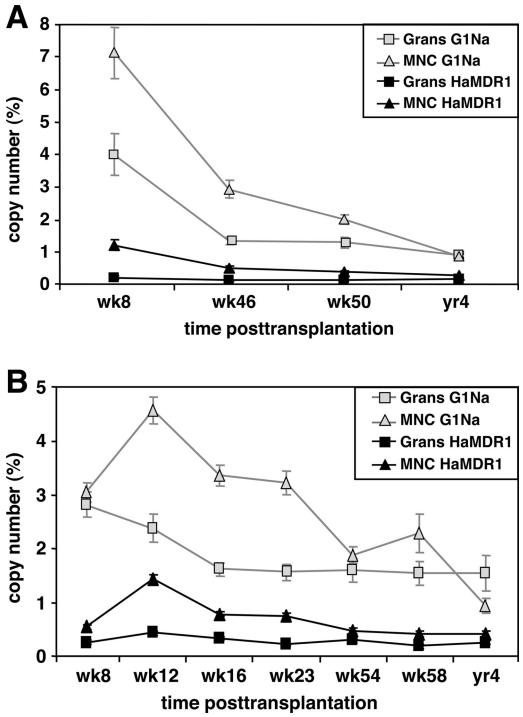

Figure 3. Percentage of transgene-positive DNA at different time points after transplantation. **(A):** Monkey M120; **(B):** Monkey M038. The values represent the percentage of vector-positive DNA measured in a sample. The rhesus macaque β2-microblobulin (*rhB2M*) gene was used to measure the total amount of DNA deployed in one experiment (*rhB2M* copy number = 100%). The copy numbers measured for each vector were then related to the *rhB2M* copy number and are displayed as percentages of total DNA. The error bars represent the SEM. Abbreviations: Grans, granulocytes; MNC, mononuclear cell; wk, week; yr, year.

Biosystems (User's Manual, ABI Prism 7700 Sequence Detection System). The mean intraexperimental/interexperimental coefficients of variation of the assay for the quantitation of the *rhB2M, NeoR*, and *MDR1* genes were 0.19/0.22, 0.12/0.15, and 0.18/0.27, respectively.

The mean PCR efficiencies for the primer pair that amplified the *rhB2M*, *NeoR*, and *MDR1* genes were 89.21% ± 0.84%, 88.65% ± 0.91%, and 81.48% ± 1.05%, respectively. This would mean that all *MDR1* figures are approximately 10% too low compared with the *NeoR* and *rhB2M* figures. However, this deviation remains in the scope of the SEM of the *MDR1* figures, and thus this difference is not statistically significant.

The contribution of each vector transgene at different time points is shown in Figure 3A (M120) and 3B (M038). Eight weeks after transplantation, the percentages of *G1Na*-positive DNA in the granulocyte and MNC fractions for monkey M120 were 4.05% ± 0.63% and 7.18% ± 0.78%, respectively, descending to contribution levels at approximately 1% 4 years post-transplantation (Fig. 3A). In monkey M038, the percentage of *G1Na*-positive granulocyte DNA declined from 2.82% ± 0.24% 8 weeks after transplantation to 1.62% ± 0.12% 16 weeks after transplantation and was virtually constant at a level around 1.5% after week 16 (Fig. 3B). Although the data of MNCs show more fluctuations for monkey M038, the tendency is the same as in monkey M120: a decline of the percentages of *G1Na*-positive DNA from 4.57% ± 0.24% after 12 weeks to 0.93% ± 0.14% after 4 years. The percentage of *HaMDR1*-positive granulocyte DNA was at a constant level of less than 1% for 4 years in both monkeys (range, 0.18% ± 0.02% to 0.27% ± 0.05% in monkey M120 and 0.43% ± 0.05% to 0.19% ± 0.04% in monkey M038); the percentage of *HaMDR1*-transduced MNCs declined from an initial value of approximately 1.5% and converged thereafter to the granulocyte level in both monkeys (range, 1.26% ± 0.16% to 0.34% ± 0.04% in monkey M120 and 1.42% ± 0.09% to 0.40% ± 0.06% in monkey M038) (Fig. 3A, 3B).

Quantitation of Contributions of Single Clones

To measure the contribution of individual transgene-marked CD34+ cells to hematopoiesis, we performed QRT-PCR on single clones. The validation of this method for the approach of quantification of single clones was performed by quantifying an individual plasmid in a plasmid mixture [29]. Three plasmids containing different LM-PCR product were mixed in certain ratios, and then the proportion of an individual plasmid was quantified. Nagy et al. [29] were able to detect the proportion of an individual plasmid down to 10 copies in a total plasmid number of 10^5. The mean intraexperimental and interexperimental coefficients of variation of our assay for the quantitation of the single clones were 0.41 and 0.35, respectively. This loss of precision in the quantitation of such low values is explained by the actual principle of the PCR methodology, with a variation as low as 1 Ct, leading to 100% variation in the final quantification. Considering this, it is important to emphasize that the use of QRT-PCR at such low quantities is only suitable to measure a range of values for a clone in which it most likely appears. Furthermore, since in some cases the Ct values of the samples approached the no-amplification Ct value of 45, we included only reactions in which the NTC and the NAC were absolutely negative with a Ct value of 45.

The mean PCR efficiency for the clones was 83.76% ± 1.06% (range, 79.54% to 87.69%); the deviation of approximately 10% remains in the scope of the SEM. Thus, the PCR efficiencies allow a direct comparison of the copy numbers. Repression of the PCR efficiency due to nonspecific retroviral common primer annealing was excluded using a clone-specific primer and probe set for clone 1. The PCR efficiency for this individual set was 84.37% ± 2.11%; the correlation coefficient of the standard curve was 0.99. The clone could not be detected with this specific set.

We analyzed 18 (16 *G1Na* and 2 *HaMDR1* clones) of the 24 clones identified in both monkeys 4 years after transplantation. The remaining six clones could not be quantified because of difficulty identifying non-cross-reacting primers. The quantitation of clones found at earlier time points was not possible because of limited DNA availability.

Ten of the 16 *G1Na* clones analyzed were not detectable and thus contributed at levels less than the QRT-PCR detection limit of 0.0001% [29]. The remaining six clones had copy numbers between 1.43 ± 0.52 and 7.1 ± 0.34, equivalent to 0.09% ± 0.03% and 0.42% ± 0.03% of *G1Na*-positive DNA. Two *HaMDR1* clones were analyzed, showing copy numbers of 3.52 ± 1.11 and 2.87 ± 0.56, respectively, equivalent to 0.71% ± 0.23% and 0.84% ± 0.2% of *HaMDR1*-positive DNA. An overview of the proportion of all quantified clones is given in Table 2. The individual clones contributed at levels of 0.0008% ± 0.0003% to 0.0041% ± 0.00032% to the total primate hematopoiesis, calculated on the basis of *rhB2M* gene copies (Table 2; Fig. 4).

Integration Analysis

We performed genomic mapping of 122 integration sites. Seventy-two *G1Na* and 15 *MDR1* clones could be mapped successfully (supplemental online Table 2), whereas 35 clones contained too many repetitive elements and thus could not be identified in the human genome. The *G1Na* vector showed

Table 2. Proportion of individual clones identified 4 years after transplantation

Monkey/cell type	Template/clone	Copy number (absolute)	Copy number (% of proviral DNA)	Copy number (% of all DNA in sample)
M120	rhB2M	172,849.7 ± 10,740.8	—[a]	100
Granulocytes	NeoR	1,675.7 ± 68.5	100	0.97 ± 0.08
	1	2.25 ± 0.55	0.13 ± 0.03	0.0013 ± 0.00033
	2	7.1 ± 0.34	0.42 ± 0.03	0.0041 ± 0.00032
	3	3.91 ± 0.67	0.23 ± 0.04	0.0023 ± 0.00041
	4[b]	7.02 ± 0.82	0.42 ± 0.05	0.0041 ± 0.00054
	5	1.43 ± 0.52	0.09 ± 0.03	0.0008 ± 0.00031
	6	2.53 ± 0.54	0.15 ± 0.03	0.0015 ± 0.00033
	7	Not detected	—	—
M120	rhB2M	148,923.6 ± 20,813.3	—	100
MNCs	MDR1	497.9 ± 50.2	100	0.23 ± 0.03
	8	3.52 ± 1.11	0.71 ± 0.23	0.0024 ± 0.0008
	G1Na clones 9–14	Not detected	—	—
M038	rhB2M	130,157.5 ± 15,389.9	—	100
Granulocytes	MDR1	339.8 ± 43.2	100	0.26 ± 0.03
	15[c]	2.87 ± 0.56	0.84 ± 0.2	0.0022 ± 0.00067
	G1Na clone 16	Not detected	—	—

[a]—, not applicable.
[b]Integration in gene *LOC201895*.
[c]Integration in gene *SIN3A*.

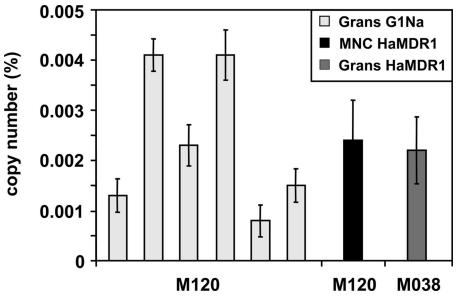

Figure 4. Percentages of quantified single clones 4 years after transplantation relating to *rhB2M*. Each column represents an individual clone. The values graph the copy numbers of individual clones relating to the rhB2M copy number (rhB2M copy number = 100%) displayed in the last column of Table 2. The error bars represent the SEM calculated from the means of the PCR triplicates. *G1Na* clones in the MNC fraction were not detectable in either monkey. Abbreviations: Grans, granulocytes; MNC, mononuclear cell.

preferential integrations in RefSeq genes (48%), near transcription start sites of genes (37%) and within a range of ±200 base pairs to SINEs (38%) and LINEs (18%). In addition, a significantly elevated retroviral insertion estimate into chromosome (RISC) score [26] (RISC = 9; $p < .05$) for chromosome 19 was observed (data not shown). Of the *HaMDR1* integrations, 73% were found in RefSeq genes.

We found five integrations in gene loci involved in malignant transformation of cells, three times with the *G1Na vector* and two times with the *HaMDR1* vector. One integration of the *G1Na* vector occurred in the *TIAM1* (T-cell lymphoma invasion and metastasis one) oncogene, one in the *SKI* (v-ski sarcoma viral oncogene homolog) transcript and one in the *Evi1* (ecotropic virus integration site one) gene. One integration of the *HaMDR1* vector in the *MECT1* (mucoepidermoid carcinoma translocated 1 isoform) gene and one in the transcription regulating gene *SIN3A* (transcriptional corepressor *Sin3A*) were found.

Analysis regarding clone size, vector, and integration site did not reveal any correlations: 4 of the 18 clones quantified occurred in RefSeq genes. These genes were the *STK10* (serine/threonine kinase 10) gene; the *CYP7B1* (cytochrome P450 family seven subfamily B) gene; the *LOC201895* (hypothetical protein LOC201895) gene, hit by the *G1Na* vector; and the *SIN3A* gene, hit by the *HaMDR1* vector. Although the clones carrying the insertion sites in the *STK10* and the *CYP7B1* genes were too small to be detected, the contribution of the *LOC201895* clone and the *SIN3A* clone to rhesus macaque hematopoiesis was 0.0041% ± 0.00054% and 0.0022% ± 0.00067%, respectively (Table 2). The contribution of the *SIN3A* clone was comparable to the contribution of the clones containing integrations other than in genes or oncogenes (Table 2).

Discussion

We analyzed the contribution of gene-modified CD34+ cells in two monkeys from 8 weeks up to 4 years after transplantation. This is the longest study period of *MDR1*-transduced cells in rhesus monkeys or other primates reported so far.

Number of Clones Descending from G1Na and HaMDR1-Transduced Cells

We found a total of 122 different contributing clones in granulocytes and mononuclear cells from 8 weeks up to 4 years after reinfusion of gene-modified CD34+ cells. One hundred two clones descend from the *G1Na* vector and only 20 from the *HaMDR1* vector (Table 1). Using EFRAM-PCR, we were able to detect integration sites using very small amounts of DNA (100 ng). In contrast to LM-PCR, in which fragments are biotin-linked in a one-step amplification reaction, or to linear amplification-mediated PCR (LAM-PCR) [38], which uses linear biotin marking of DNA fragments, the fragments are biotin-marked and amplified simultaneously in EFRAM-PCR. Using this new method, we could reduce the amount of starting DNA from 2,500 ng needed for LM-PCR to 100 ng in EFRAM-PCR. Thus, EFRAM-PCR is a highly sensitive method applicable for samples containing only few transduced cells and in situations in which only small amounts of DNA are available.

Since the efficiency of enrichment of fragments using paramagnetic beads depends on the fragment size (as provided by the manufacturer), we used primers that aligned to both vectors and led to amplification of LTR sequences of equal length, so

that the chance for each vector to be detected by LM-PCR was equal. Thus, a methodical advantage for the *G1Na* vector during detection of the two vectors as the underlying reason for the higher *G1Na* clone count can be excluded.

Another reason for the difference in the number of identified clones could be a difference in the number of transduced cells. The ratio of *HaMDR1*-transduced to *G1Na*-transduced cells was 1/1.18 (40/47) for monkey M038 and 1/1.81 (37/67) for monkey M120 [24]. One would expect similar ratios for the number of clones, assuming similar engraftment levels for both vectors. However, the ratio of identified *HaMDR1* clones to *G1Na* clones was much higher, 1/3.6 in monkey M038 and 1/7.4 in monkey M120; thus, four times as many *G1Na* clones were found as expected. The discrepancy between the ratio of transduced cells and the ratio of identified clones could be due to a smaller overall contribution of *HaMDR1*-transduced cells to hematopoiesis. To investigate this, we performed QRT-PCR to measure the contribution of all transduced cells and single transduced cells to hematopoiesis.

Contribution of the G1Na and HaMDR1 Vectors to Hematopoiesis

In both monkeys, the percentage of *G1Na*-positive DNA was initially high, between 4% and 7%, 8 weeks after transplantation and declined to contribution levels of approximately 1%, whereas the percentage of *HaMDR1*-positive DNA remained constantly less than 1% over the whole observation period (Fig. 3A, 3B).

Since transduction efficiency was similar for both vectors in both monkeys [24], it remains unclear why the percentage of *G1Na*-positive DNA is constantly higher than the percentage of *HaMDR1*-positive DNA. One reason could be technical issues during the transduction process, such as toxicity of supernatants or reduced gene transfer rate because of high numbers of virus-like particles. Biological reasons for the reduced marking rates could be both a selective disadvantage of *HaMDR1*-transduced cells upon engraftment and reduced proliferation or release into the peripheral blood, depending on *MDR1* expression. However, if *MDR1* expression in rhesus hematopoiesis confers a selective disadvantage, the clones persisting long-term may have been selected to escape MDR1 overexpression. In addition to epigenetic silencing, ectopic *MDR1* expression may also be abrogated by instability of the vector genome [39, 40]. Proof of *MDR1* expression in vivo was obtained for monkey M038 at week 27 and for monkey M120 at week 20 [24]. Since only genomic DNA was available to us, we could not perform expression analysis at later time points. Therefore, the conclusions drawn in this study point out that the transduction itself did not lead to clonal dominance. A proof of *MDR1* expression would be essential in the investigation of proliferative advantage after application of chemotherapy.

The decrease of *G1Na* marking rates over 4 years can be interpreted either as a negative selective pressure on *G1Na* vector-transduced cells or as a positive selective pressure on *HaMDR1*-transduced cells. Although the *MDR1* vector increases, relative to the control vector, potentially showing a selective advantage of *HaMDR1*-transduced cells, a selective negative pressure on *G1Na* vector-transduced cells is rather likely, since earlier studies showed that positive selective pressure on *MDR1*-transduced cells results in an increase of marking rates [4] because of the fact that contribution levels of *HaMDR1*-transduced cells remain constant over 4 years. This suggestion is corroborated by a recent study in which integration of the *NeoR* gene-carrying vector did not remain silent but also altered the gene expression pattern of transduced cells [41], as shown for other vectors containing control transgenes such as green fluorescent protein (*GFP*) [42]. An approach for future trials to overcome this experimental source of error could be the use of a control vector containing the inverted transgene.

Thus, in both monkeys, there were no indications for a misregulated proliferation of *HaMDR1*-positive cells after 4 years, which would be apparent in an increase of the percentages. In contrast, the stable contribution of *HaMDR1*-positive HSCs to hematopoiesis implies normal cell behavior.

The higher contribution of *G1Na*-transduced cells explains the higher number of identified *G1Na* clones. To further investigate the contribution of these clones on a quantitative level, we performed QRT-PCR on 18 clones (16 *G1Na* and 2 *HaMDR1* clones) identified in both monkeys 4 years after transplantation.

Contribution of Individual Clones to Hematopoiesis

Compared with earlier studies with a time frame of only 6–8 weeks [29] or the analysis of exclusively one integration site [37], this is the first time that the contribution of multiple distinct single transduced repopulating cells is quantified after a long-term follow-up. To rule out repression of the PCR efficiency due to nonspecific retroviral common primer annealing, we chose to analyze clone 1, one of the smallest clones, with an individual primer and probe set. Assuming that there is an efficiency problem due to nonspecific primer binding, a small clone should be measured with a bigger clone size if analyzed with a clone-specific primer and probe set. However, multiple QRT-PCR analyses using this specific set, including the use of different clone-specific reverse primers, could not detect this clone. Thus, the clone-specific set was less sensitive than the vector-specific set with a clone-specific reverse primer, ruling out a limitation factor due to nonspecific primer annealing in the measurement of clone sizes in this setting.

Ten of the clones analyzed were not detectable and thus were under the QRT-PCR detection limit of 0.0001% [29], pointing to extremely small copy numbers. Six *G1Na* clones could be quantified, showing a clonal size of 0.09% ± 0.03% to 0.42% ± 0.03% of *G1Na*-transduced PBCs; the two *HaMDR1* clones showed a clonal size of 0.71% ± 0.23% and 0.84% ± 0.2% of *HaMDR1*-transduced PBCs (Table 2). The eight clones contributed to total primate hematopoiesis at levels of 0.0008% ± 0.0003% to 0.0041% ± 0.00032% (Table 2; Fig. 4), also showing that our assay had a high sensitivity for the detection of individual clone sizes. We found no dominant clone or clonal expansion of either *G1Na*- or *HaMDR1*-transduced cell clones. However, these data have to be regarded with caution, as only a small number of *HaMDR1* clones could be identified and quantified, despite a maximum effort to retrieve from fresh and archival material available from these monkeys. Thus, these data are rather an indication of normal behavior of *HaMDR1* clones, given the stable overall contribution of *HaMDR1*-transduced cells. Furthermore, we cannot rule out that some clones may have escaped detection for technical reasons (e.g., size or secondary structure of the PCR product). Additional biostatistical analyses of clonal dynamics were not performed, as this would require time course data of clonal contribution for at least 3–5 quantified clones per vector type. Also, a statistical confirmation of a difference of, for example, 10% in the frequency of dominant clones between these groups on the basis of Fisher's exact test with a given significance level of 5% and a power of 80% requires at least 170 quantified clones for each vector [32]. These numbers cannot be achieved with the DNA amounts available to us.

To assess and predict clonal behavior and potential clonal dominance (e.g., by the use of quantitative modeling approaches [43, 44]), it is of high interest to quantify the contribution of

distinct clones over a prolonged period of time. Currently, unfortunately, a large amount of DNA for quantitation of a clone is needed. This large amount of DNA is often not available. During the experimental phase of this study, there was no possibility to quantify clones at other time points than 4 years after transplantation because of limited DNA amounts available from earlier time points.

Integration in Oncogenes Without Incidence of Leukemia

The *G1Na* vector showed preferential integrations in RefSeq genes, near transcription start sites of genes, SINEs, and LINEs. Furthermore, a significantly elevated RISC score [26] (RISC = 9, $p < .05$) for chromosome 19 was observed. These findings are in line with patterns observed in other *MLV* vector-based studies [45, 46]. Of the *HaMDR1* integrations, 73% were found in RefSeq genes. Yet, because of the small number of mapped *HaMDR1* integration sites, this finding cannot be judged as a statistically significant preference.

We found an integration of the *G1Na* vector in the *Evi1* gene in monkey M038 58 weeks after transplantation, without the evidence of an abnormal increase of *G1Na*-positive DNA in the QRT-PCR analysis (Fig. 3B) [37], whereas earlier integration studies observed development of leukemia in mice after vector integration in this proto-oncogene [47].

We did not observe any correlation among clone size, vector, and integration site. The contribution of the *SIN3A* clone was comparable to the contribution of the clones containing integrations other than in genes or oncogenes. In addition, the overall contribution of *HaMDR1*-transduced cells to hematopoiesis remained less than 1%. Thus, to date there is no indication that *HaMDR1* integrations in the *SIN3A* and *MECT1* oncogenes caused uncontrolled proliferative behavior. Taken together, our data support the assumption that an integration in a single oncogene cannot be solely responsible for causing malignant transformation of a cell [37, 48, 49].

Summary

With this study, we were able to show that *HaMDR*1- and *G1Na*-transduced CD34+ cells contributed to hematopoiesis on a stable level without indication of clonal dominance over a prolonged follow-up period. Integrations occurring into an oncogene did not lead to leukemic proliferation of transduced cells after 4 years of follow-up.

The myeloproliferative disorder of *HaMDR1*-transduced cells observed in earlier studies in mice [21, 22] was most likely due to multiple integrations of the vector in one cell, as shown in a recent study [49]. Clinically effective transduction and transplantation protocols [18], as well as new vectors [50, 51], are now required to test the efficacy of *MDR1* gene therapy and in vivo chemoselection in a clinical setting.

Acknowledgments

The technical assistance of Bernard Berkus, Hans-Jürgen Engel, Sigrid Heil (German Cancer Research Center), and Carmen Hoppstock (University of Heidelberg) are gratefully acknowledged. We also thank Luisa Schubert (German Cancer Research Center) for assistance with LM-PCR. We are most grateful to the German Primate Center for providing untransduced rhesus macaque DNA. Special thanks are due to Marlon Veldweijk and Uwe Appelt (German Cancer Research Center) for advice on data analysis. This work was supported by grants FR 1732/3-1 and RO-3500/1-1 of the Deutsche Forschungsgemeinschaft. F.B. and S.L. contributed equally to this work.

Disclosure of Potential Conflicts of Interest

The authors indicate no potential conflicts of interest.

References

1 Goldspiel BR. Chemotherapy dose density in early-stage breast cancer and non-Hodgkin's lymphoma. Pharmacotherapy 2004;24:1347–1357.
2 Fruehauf S, Breems DA, Knaan-Shanzer S et al. Frequency analysis of multidrug resistance-1 gene transfer into human primitive hematopoietic progenitor cells using the cobblestone area-forming cell assay and detection of vector-mediated P-glycoprotein expression by rhodamine-123. Hum Gene Ther 1996;7:1219–1231.
3 Schiedlmeier B, Kuhlcke K, Eckert HG et al. Quantitative assessment of retroviral transfer of the human multidrug resistance 1 gene to human mobilized peripheral blood progenitor cells engrafted in nonobese diabetic/severe combined immunodeficient mice. Blood 2000; 95:1237–1248.
4 Schiedlmeier B, Schilz AJ, Kuhlcke K et al. Multidrug resistance 1 gene transfer can confer chemoprotection to human peripheral blood progenitor cells engrafted in immunodeficient mice. Hum Gene Ther 2002;13: 233–242.
5 Neff T, Beard BC, Peterson LJ et al. Polyclonal chemoprotection against temozolomide in a large-animal model of drug resistance gene therapy. Blood 2005;105:997–1002.
6 Ueda K, Cornwell MM, Gottesman MM et al. The mdr1 gene, responsible for multidrug-resistance, codes for P-glycoprotein. Biochem Biophys Res Commun 1986;141:956–962.
7 Mulder HS, Dekker H, Pinedo HM et al. The P-glycoprotein-mediated relative decrease in cytosolic free drug concentration is similar for several anthracyclines with varying lipophilicity. Biochem Pharmacol 1995;50:967–974.
8 Illmer T, Schaich M, Platzbecker U et al. P-glycoprotein-mediated drug efflux is a resistance mechanism of chronic myelogenous leukemia cells to treatment with imatinib mesylate. Leukemia 2004;18:401–408.
9 Radujkovic A, Schad M, Topaly J et al. Synergistic activity of imatinib and 17-AAG in imatinib-resistant CML cells overexpressing BCR-ABL: Inhibition of P-glycoprotein function by 17-AAG. Leukemia 2005;19: 1198–1206.
10 Galski H, Sullivan M, Willingham MC et al. Expression of a human multidrug resistance cDNA (MDR1) in the bone marrow of transgenic mice: Resistance to daunomycin-induced leukopenia. Mol Cell Biol 1989;9:4357–4363.
11 Mickisch GH, Licht T, Merlino GT et al. Chemotherapy and chemosensitization of transgenic mice which express the human multidrug resistance gene in bone marrow: Efficacy, potency, and toxicity. Cancer Res 1991;51:5417–5424.
12 Hanania EG, Giles RE, Kavanagh J et al. Results of MDR-1 vector modification trial indicate that granulocyte/macrophage colony-forming unit cells do not contribute to posttransplant hematopoietic recovery following intensive systemic therapy. Proc Natl Acad Sci U S A 1996; 93:15346–15351.
13 Hesdorffer C, Ayello J, Ward M et al. Phase I trial of retroviral-mediated transfer of the human MDR1 gene as marrow chemoprotection in patients undergoing high-dose chemotherapy and autologous stem-cell transplantation. J Clin Oncol 1998;16:165–172.
14 Devereux S, Corney C, Macdonald C et al. Feasibility of multidrug resistance (MDR-1) gene transfer in patients undergoing high-dose therapy and peripheral blood stem cell transplantation for lymphoma. Gene Ther 1998;5:403–408.
15 Cowan KH, Moscow JA, Huang H et al. Paclitaxel chemotherapy after autologous stem-cell transplantation and engraftment of hematopoietic cells transduced with a retrovirus containing the multidrug resistance complementary DNA (MDR1) in metastatic breast cancer patients. Clin Cancer Res 1999;5:1619–1628.
16 Moscow JA, Huang H, Carter C et al. Engraftment of MDR1 and NeoR gene-transduced hematopoietic cells after breast cancer chemotherapy. Blood 1999;94:52–61.
17 Abonour R, Williams DA, Einhorn L et al. Efficient retrovirus-mediated

transfer of the multidrug resistance 1 gene into autologous human long-term repopulating hematopoietic stem cells. Nat Med 2000;6:652–658.
18 Cavazzana-Calvo M, Fischer A. Efficacy of gene therapy for SCID is being confirmed. Lancet 2004;364:2155–2156.
19 Aiuti A. Gene therapy for adenosine-deaminase-deficient severe combined immunodeficiency. Best Pract Res Clin Haematol 2004;17: 505–516.
20 Ott MG, Schmidt M, Schwarzwaelder K et al. Correction of X-linked chronic granulomatous disease by gene therapy, augmented by insertional activation of MDS1-EVI1, PRDM16 or SETBP1. Nat Med 2006; 12:401–409.
21 Bunting KD, Zhou S, Lu T et al. Enforced P-glycoprotein pump function in murine bone marrow cells results in expansion of side population stem cells in vitro and repopulating cells in vivo. Blood 2000;96:902–909.
22 Bunting KD, Galipeau J, Topham D et al. Transduction of murine bone marrow cells with an MDR1 vector enables ex vivo stem cell expansion, but these expanded grafts cause a myeloproliferative syndrome in transplanted mice. Blood 1998;92:2269–2279.
23 Baum C, von Kalle C, Staal FJT et al. Chance or necessity? Insertional mutagenesis in gene therapy and its consequences. Mol Ther 2004;9:5–13.
24 Sellers SE, Tisdale JF, Agricola BA et al. The effect of multidrug-resistance 1 gene versus neo transduction on ex vivo and in vivo expansion of rhesus macaque hematopoietic repopulating cells. Blood 2001;97:1888–1891.
25 Heid CA, Stevens J, Livak KJ et al. Real time quantitative PCR. Genome Res 1996;6:986–994.
26 Laufs S, Gentner B, Nagy KZ et al. Retroviral vector integration occurs in preferred genomic targets of human bone marrow-repopulating cells. Blood 2003;101:2191–2198.
27 Giordano FA, Hotz-Wagenblatt A, Lauterborn D et al. New bioinformatic strategies to rapidly characterize retroviral integration sites of gene therapy vectors. Methods Inf Med 2007, in press.
28 Del Val C, Glatting KH, Suhai S. cDNA2Genome: A tool for mapping and annotating cDNAs. BMC Bioinformatics 2003;4:39.
29 Nagy KZ, Laufs S, Gentner B et al. Clonal analysis of individual marrow-repopulating cells after experimental peripheral blood progenitor cell transplantation. STEM CELLS 2004;22:570–579.
30 Baum C, Hegewisch-Becker S, Eckert HG et al. Novel retroviral vectors for efficient expression of the multidrug resistance (mdr-1) gene in early hematopoietic cells. J Virol 1995;69:7541–7547.
31 Su J, Luscher M, MacDonald K. Sequence of beta(2)-microglobulin from rhesus macaque (Macaca mulatta) includes an allelic variation in the 3′-untranslated region. Immunogenetics 2004;55:873–877.
32 Sachs L. Angewandte Statistik, 10th ed. Springer, 2002:159–161.
33 Kiem HP, Allen J, Trobridge G et al. Foamy virus-mediated gene transfer to canine repopulating cells. Blood 2007;109:65–70.
34 Venditti G, Di Ianni M, Falzetti F et al. NeoR-based transduced T lymphocytes detected by real-time quantitative polymerase chain reaction. J Hematother Stem Cell Res 2003;12:83–91.
35 Becker K, Pan D, Whitley CB. Real-time quantitative polymerase chain reaction to assess gene transfer. Hum Gene Ther 1999;10:2559–2566.
36 Gerard CJ, Arboleda MJ, Solar G et al. A rapid and quantitative assay to estimate gene transfer into retrovirally transduced hematopoietic stem/progenitor cells using a 96-well format PCR and fluorescent detection system universal for MMLV-based proviruses. Hum Gene Ther 1996;7: 343–354.
37 Calmels B, Ferguson C, Laukkanen MO et al. Recurrent retroviral vector integration at the Mds1/Evi1 locus in nonhuman primate hematopoietic cells. Blood 2005;106:2530–2533.
38 Schmidt M, Zickler P, Hoffmann G et al. Polyclonal long-term repopulating stem cell clones in a primate model. Blood 2002;100:2737–2743.
39 Kimchi-Sarfaty C, Oh JM, Kim IW et al. A "silent" polymorphism in the MDR1 gene changes substrate specificity. Science 2007;315:525–528.
40 Cmejlova J, Hildinger M, Cmejla R et al. Impact of splice-site mutations of the human MDR1 cDNA on its stability and expression following retroviral gene transfer. Gene Ther 2003;10:1061–1065.
41 Maier P, Fleckenstein K, Li L et al. Overexpression of MDR1 using a retroviral vector differentially regulates genes involved in detoxification and apoptosis and confers radioprotection. Radiat Res 2006; 166:463–473.
42 Hanazono Y, Yu JM, Dunbar CE et al. Green fluorescent protein retroviral vectors: Low titer and high recombination frequency suggest a selective disadvantage. Hum Gene Ther 1997;8:1313–1319.
43 Roeder I. Quantitative stem cell biology: Computational studies in the hematopoietic system. Curr Opin Hematol 2006;13:222–228.
44 Roeder I, Kamminga LM, Braesel K et al. Competitive clonal hematopoiesis in mouse chimeras explained by a stochastic model of stem cell organization. Blood 2005;105:609–616.
45 Hematti P, Hong BK, Ferguson C et al. Distinct genomic integration of MLV and SIV vectors in primate hematopoietic stem and progenitor cells. PLoS Biol 2004;2:e423.
46 Laufs S, Nagy KZ, Giordano FA et al. Insertion of retroviral vectors in NOD/SCID repopulating human peripheral blood progenitor cells occurs preferentially in the vicinity of transcription start regions and in introns. Mol Ther 2004;10:874–881.
47 Li Z, Dullmann J, Schiedlmeier B et al. Murine leukemia induced by retroviral gene marking. Science 2002;296:497.
48 Seggewiss R, Pittaluga S, Adler RL et al. Acute myeloid leukemia associated with retroviral gene transfer to hematopoietic progenitor cells of a rhesus macaque. Blood 2006;2005–2010.
49 Modlich U, Kustikova OS, Schmidt M et al. Leukemias following retroviral transfer of multidrug resistance 1 (MDR1) are driven by combinatorial insertional mutagenesis. Blood 2005;105:4235–4246.
50 Vigna E, Amendola M, Benedicenti F et al. Efficient Tet-dependent expression of human factor IX in vivo by a new self-regulating lentiviral vector. Mol Ther 2005;11:763–775.
51 Baum C, Kustikova O, Modlich U et al. Mutagenesis and oncogenesis by chromosomal insertion of gene transfer vectors. Hum Gene Ther 2006; 17:253–263.

See www.StemCells.com for supplemental material available online.

No Evidence of Clonal Dominance in Primates up to 4 Years Following Transplantation of Multidrug Resistance 1 Retrovirally Transduced Long-Term Repopulating Cells

Farastuk Bozorgmehr, Stefanie Laufs, Stephanie E. Sellers, Ingo Roeder, Werner J. Zeller, Cynthia E. Dunbar and Stefan Fruehauf

Stem Cells 2007;25;2610-2618; originally published online Jul 5, 2007;
DOI: 10.1634/stemcells.2007-0017